JOURNAL OF SPACECRAFT AND ROCKETS
Vol. 38, No. 4, July–August 2001

Simulating Ionospheric Plasma with a Hollow Cathode in a Large Vacuum Chamber

Sven G. Bilén*
Pennsylvania State University, University Park, Pennsylvania 16802
Matthew T. Domonkos†
NASA John H. Glenn Research Center at Lewis Field, Cleveland, Ohio 44135
and
Alec D. Gallimore‡
University of Michigan, Ann Arbor, Michigan 48109

A plasma environment closely approximating the ionosphere can be generated by a hollow cathode assembly in a large vacuum chamber. This capability allows examinations of ionospheric-plasma phenomena in a controlled setting without, in most cases, relying on scaling techniques. The hollow cathode provides a low-temperature, low-density, fairly uniform plasma in its far field, and the large chamber provides ample room such that the effects of plasma confinement are reduced to a minimum. Most previous studies of hollow cathodes have concentrated on their plasma environment in the near field, i.e., within a few tens of centimeters. This work, however, examines their far-field plasma environment, i.e., 1–2 m. This characterization shows that the hollow cathode provides, in the far field, a fairly uniform ionospheric-level plasma environment. The hollow cathode was operated at nine different operating conditions consisting of three different gases (argon, krypton, and xenon) each at three different flow rates. Results from these nine operating conditions are summarized, and the corresponding far-field plasma environments are analyzed. Comparison of the hollow cathode's plasma environment parameters with typical ionospheric values is presented. Uses of the facility, such as full-scale scientific instrument verification, are presented.

Nomenclature

B_E	=	geomagnetic-flux density, T
$\boldsymbol{B}_E$	=	geomagnetic-flux-density vector, T
B_0	=	background magnetic-flux density, T
$\boldsymbol{B}_{\text{IGRF}}$	=	magnetic-flux density from IGRF model, T
$\boldsymbol{B}_{\text{LVTF}}$	=	magnetic-flux density in LVTF, T
k	=	Boltzmann's constant, 1.38×10^{-23} J/K
m_e	=	electron mass, 9.109×10^{-31} kg
m_i	=	ion mass, kg
n_e	=	electron plasma density, m^{-3}
n_i	=	ion density, m^{-3}
q	=	charge magnitude, 1.602×10^{-19} C
r_{ce}	=	electron gyroradius, m
r_{ci}	=	ion gyroradius, m
T_e	=	electron temperature, K
v_{te}	=	electron thermal velocity, m/s
v_{ti}	=	ion thermal velocity, m/s
Z_i	=	ionization level, integer
ε_0	=	free space permittivity, 8.85×10^{-12} F/m
θ_e	=	electron temperature, eV

Introduction

THE capability of generating a plasma environment that closely approximates that of the ionosphere is highly desirable to researchers wishing to examine ionospheric-plasma phenomena in a controlled setting. Such a capability would also be useful in testing and calibrating ionospheric probes without relying on scaling techniques.[1] The use of a hollow cathode assembly (HCA) in a large vacuum chamber, such as the University of Michigan's Large Vacuum Test Facility (LVTF), can provide just such a capability. The HCA provides a low-temperature, low-density, fairly uniform plasma in its far field, and the LVTF provides ample room such that the effects of plasma confinement (i.e., interaction with the walls and support structures) can be reduced to a minimum.

The general operation of HCAs has been studied extensively in the literature.[2–6] Many previous studies of the HCA have concentrated on its plasma environment in the near field, i.e., within a few tens of centimeters.[6,7] Several works have also investigated the interaction of the HCA plume with an ambient plasma,[8–11] although this is not the case of this study. Rather, this work examines the far-field (i.e., ~1–2-m) plasma environment of the HCA. This characterization shows that the HCA provides, in the far field, a fairly uniform ionospheric-level plasma environment.

The HCA was operated at a total of nine different operating conditions: three different gases (argon, krypton, and xenon), each at three different flow rates. In this paper we begin with a description of the vacuum chamber and experimental apparatus. We then present and summarize the results from the nine operating conditions and analyze the corresponding far-field plasma environments. We conclude by presenting an evaluation of our method and apparatus for simulating ionospheric plasmas and its utility. We also present several possible uses for our method, highlighting appropriate uses.

Experimental Apparatus

Vacuum Chamber Description

The University of Michigan's Plasmadynamics and Electric Propulsion Laboratory has as its centerpiece the LVTF, a cylindrical, stainless-steel-clad tank, which is 9 m long and 6 m in diameter.[12] During these tests, the vacuum was generated by six 32,000-l/s diffusion pumps backed by two 56,600-l/s blowers and four 11,300-l/s mechanical pumps. These pumps gave the facility an overall pumping speed of over 100,000 l/s on nitrogen and 25,000 l/s on xenon at high vacuum. In Winter 1998 the LVTF underwent a major facilities upgrade during which four reentrant (nude) cryopumps were added. These cryopumps have a combined pumping speed of 300,000 l/s on air and 140,000 l/s on xenon and provide the ability to reach a high-vacuum (10^{-7} torr). Figure 1 is a diagram of the LVTF as it was set up for the HCA far-field plasma-environment characterization.

Received 8 October 1999; revision received 17 November 2000; accepted for publication 22 November 2000.

*Assistant Professor, Electrical Engineering and Engineering Design and Graphics. Member AIAA.
†Aerospace Engineer, Onboard Propulsion Branch. Member AIAA.
‡Associate Professor, Aerospace Engineering and Applied Physics. Associate Fellow AIAA.

Table 1 Summary of the operating conditions of the HCA

Operating condition	Gas	Flow rate, sccm	Discharge voltage, V	Discharge current, A	Mode of operation[16]	Tank pressure, $\times 10^{-5}$ torr (indicated)
1	Krypton	10.2	14.8	3.97	Spot	4.9
2	Krypton	19.2	14.8	3.97	Spot	4.9
3	Krypton	4.3	19.3	3.97	Plume	4.9
4	Argon	12.9	17.2	3.97	Spot	4.9
5	Argon	18.3	15.8	3.97	Spot	5.2
6	Argon	14.8	16.5	3.97	Spot	5.1
7	Xenon	2.3	15.5	3.97	Transition	4.5
8	Xenon	6.9	14.8	3.97	Spot	5.2
9	Xenon	3.9	17.1	3.97	Transition	4.8

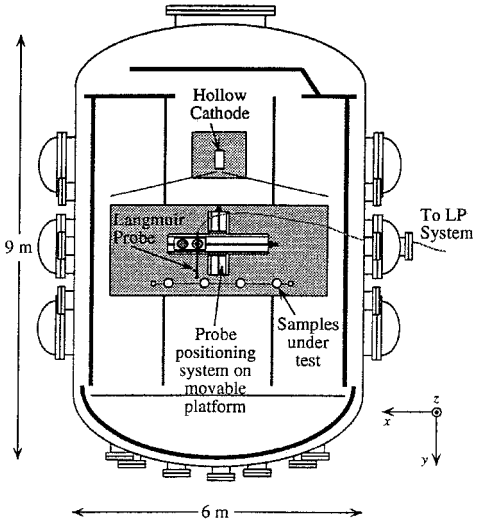

Fig. 1 Setup of the vacuum chamber for the far-field plasma environment characterization of the HCA showing the location of the HCA and the Langmuir probe mounted on the positioning table. The items marked "Samples under test" are for a different set of experiments that the HCA characterization supported.

The positioning table, also shown in Fig. 1, contains two rotary platforms on two transverse linear stages. This setup provides two degrees of freedom as well as angular freedom in the horizontal plane, i.e., radial (x plane), axial (y plane), and θ. Altitude (z plane) is fixed for these tests; however, the capability for z-axis motion has since been added to the positioning table. The entire system is mounted on a movable platform allowing measurements to be made throughout a large portion of the chamber.

HCA Description

The source for simulating the ionospheric plasma was a laboratory model 6.4-mm-diam (0.25 in.) HCA, which uses an orificed hollow cathode.[13] The HCA was developed at NASA John H. Glenn Research Center at Lewis Field under its International Space Station plasma contactor program. The HCA created a low-temperature plasma ($\theta_e \lesssim 1.5$ eV) by establishing a discharge between a hollow cathode chamber and a positive keeper electrode and was operated primarily in spot mode.[14] Plasma density was varied by adjusting the flow rate, although varying discharge current will also change plasma density and temperature.[15] Figure 2 shows a picture of the HCA as it looked during these tests. Table 1 (Ref. 16) gives a summary of the nine different HCA operating conditions.

Measurement Equipment

The measurement equipment used during these experiments included an electrometer-driven Langmuir-probe (LP) system, the aforementioned positioning table, and a computer controller to control the positioning table and the electrometer. A more in-depth description of the equipment may be found in Bilén et al.[17]

LP Measurement Positions

The LP measurements were made at 12 locations throughout the chamber for each of the nine HCA operating conditions. The 12 locations are shown in Fig. 3. The measurement space covers an area of about 1.4×0.7 m, with the closest measurement made about 1.2 m away from the HCA. The measurement space is oriented fairly symmetrically about the axis of the HCA plume. The location of the HCA is at the (0,0) point of Fig. 3.

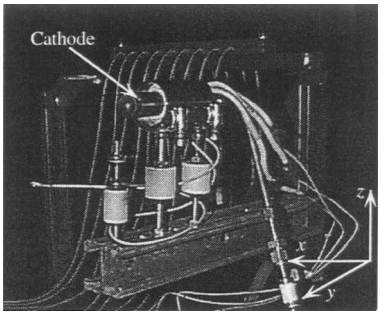

Fig. 2 Picture of the HCA as set up for these experiments. (Axis orientation shown in this figure corresponds to that of Fig. 1.)

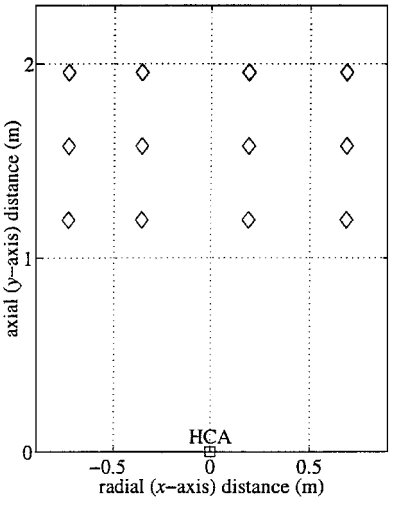

Fig. 3 Locations of the LP measurements (◇) with respect to the HCA.

Experimental Results

Plasma Measurements

The electron density throughout the measurement region was determined via the LP method as outlined in Krehbiel et al.[18] The LP bias voltage was swept from −20 to +20 V in 200 steps, and the resulting current was measured via the electrometer. The rhenium LP tip was cylindrically shaped, 48.9 mm long with a diameter of 3.9 mm, and was mounted on a triaxial mast to ensure that the low ion currents could be resolved. The probe is very similar to those used on previous ionospheric missions such as *Dynamics Explorer*, which is appropriate because of the low plasma densities of our experiment. The probe was periodically cleaned using electron bombardment of its surface by applying +200 V to the probe tip. We estimate that the error in $n_e \lesssim \pm 50\%$ and $T_e \lesssim 20\%$.

Using the n_e values obtained through analysis of the LP data, contour plots of n_e throughout the measurement region were produced for each of the nine HCA operating conditions (Table 1). A

Table 2 Summary of the plasma environment from the HCA for each of the nine operating conditions

Operating condition	Gas	Ion mass, $\times 10^{-26}$ kg	Mean n_e (std. dev.), $\times 10^{12}$ m^{-3}	Mean θ_e (std. dev.), eV	Figure number
1	Krypton	13.92	3.9 (0.9) medium	0.9 (0.1)	5
2	Krypton	13.92	11.9 (3.3) high	1.1 (0.3)	4
3	Krypton	13.92	1.2 (0.3) low	1.0 (0.2)	6
4	Argon	6.63	1.2 (0.1)	1.0 (0.2)	——
5	Argon	6.63	1.5 (0.2)	1.1 (0.3)	——
6	Argon	6.63	1.0 (0.1)	1.8 (0.2)	——
7	Xenon	21.80	1.6 (0.3)	1.5 (0.1)	——
8	Xenon	21.80	7.5 (1.7)	1.4 (0.1)	——
9	Xenon	21.80	2.9 (0.4)	1.5 (0.1)	——

Table 3 Comparison of a typical ionospheric plasma environment with that provided by the HCA in the LVTF

Parameter	Typical ionospheric value	Chamber value	Comments
n_e	10^{10}–10^{13} m^{-3}	10^{11}–10^{13} m^{-3}	Depends on distance from HCA and gas flow rate
T_e (θ_e)	1,160–3,480 K (0.1–0.3 eV)	10,400–23,100 K (0.9–2.0 eV)	Lower possibly with cold gas injection at HCA keeper
m_i (O^+)	2.66×10^{-26} kg	$\in [6.63, 13.92, 21.80] \times 10^{-26}$ kg	Other gases available, e.g., neon (3.35×10^{-26} kg)
B_E	35,000 nT (0.35 G)	~9,000 nT	Auxiliary field can be added with Helmholtz coils

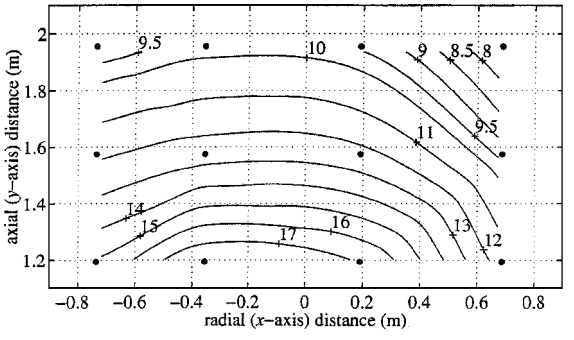

Fig. 4 Spatial distribution of high electron density (condition 2, $\times 10^{12}$ m^{-3}).

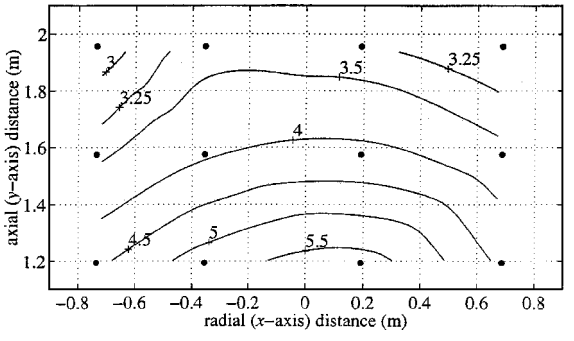

Fig. 5 Spatial distribution of medium electron density (condition 1, $\times 10^{12}$ m^{-3}).

cubic interpolation of the data collected at the 12 locations provides a smooth estimate of n_e throughout the measurement region. The plots in Figs. 4–6 show the electron density in the HCA plume for three of the nine operating conditions, which correspond to a "high," "medium," and "low" n_e case. The plots appear to have slighter higher densities to the right of the HCA, which we believe was caused by the HCA pointing slightly to the right of the center line. In addition, although the region is undersampled, fairly good density profiles can be interpolated as a result of the uniform nature of the plasma plume. Table 2 gives a summary of the plasma environments as measured by the LP.

The ion densites and electron temperatures throughout the measurement region were also determined via the LP method. The n_i values were all within a factor of 2 of n_e providing important corroboration of the results. The T_e values fell within the range 0.9–1.8 eV.

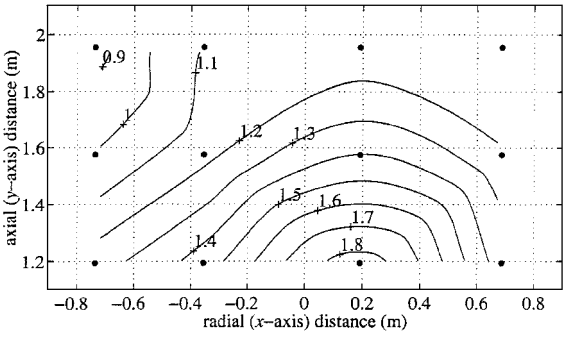

Fig. 6 Spatial distribution of low electron density (condition 3, $\times 10^{12}$ m^{-3}).

Chamber Ambient Magnetic Field

The orientation and strength of the ambient magnetic field in the chamber were measured with the Shuttle Electrodynamic Tether System[19] (SETS) aspect magnetometer (AMAG) during thermal-vacuum testing of the SETS payload on 2 February 1995. This instrument provides three-axes absolute-field measurements with 468-nT resolution. The AMAG-measured magnetic field is $\boldsymbol{B}_{\mathrm{LVTF}} = -1.83\hat{x} + 7.86\hat{y} - 4.26\hat{z} \times 10^3$ nT or $|\boldsymbol{B}_{\mathrm{LVTF}}| = 9.12 \times 10^3$ nT (coordinates are those shown in Fig. 1). Such a low value for the ambient LVTF magnetic field may at first seem incorrect because the International Geomagnetic Reference Field (IGRF) model[20] predicts a value of $|\boldsymbol{B}_{\mathrm{IGRF}}| = 5.63 \times 10^4$ nT. However, the LVTF is made of both stainless steel, which is generally nonmagnetic,[21] and ferrous steel components. The ferrous components of the LVTF affect the local field, in this case greatly reducing it. Thus, the reduction in field strength observed inside the LVTF can be explained.

Discussion

The data collected during this experiment and analyzed here show that the far-field plasma environment of the HCA approximates that of ionospheric plasmas. Table 3 compares typical values for several ionospheric parameters with those provided by the HCA in the LVTF. We discuss these and other parameters in the remainder of this section.

Plasma Density and Confinement

This characterization effort showed that the obtainable density range from the HCA in the LVTF is between ~10^{12} to 10^{13} m^{-3} and higher. This range adequately covers the higher plasma densities found in the ionosphere during daytime and/or solar maximum but is higher than those found during nighttime and/or solar minimum

Table 4 Summary of typical ionospheric and far-field HCA parameters using parameter ranges from Table 3

Parameter	Equation	Typical ionospheric values	Chamber range
ω_{pe}	$\sqrt{(n_e q^2/\varepsilon_0 m_e)}$	5.64–178 Mrad/s (0.898–28.4 MHz)	17.8–178 Mrad/s (2.84–28.4 MHz)
ω_{pi}	$\sqrt{(n_i Z_i^2 q^2/\varepsilon_0 m_i)}$	32.9–1040 krad/s (5.23–165 kHz)	Xe:36.5–Ar:661 krad/s (5.80–105 kHz)
ω_{ce}	$q B_0/m_e$	6.16 Mrad/s (908 kHz)	1.58 Mrad/s (252 kHz)
ω_{ci}	$Z_i q B_0/m_i$	209 rad/s (33.3 Hz)	Xe:6.6 rad/s (1.1 Hz), Ar:22 rad/s (3.5 Hz)
ω_{uh}	$\sqrt{(\omega_{pe}^2+\omega_{ce}^2)}$	8.35–178 Mrad/s (1.33–28.4 MHz)	17.9–178 Mrad/s (2.84–28.4 MHz)
ω_{lh}	$\approx\sqrt{(\omega_{ce}\omega_{ci})}$	35.9 krad/s (5.71 kHz)	5.9 krad/s (938 Hz)
λ_D	$\sqrt{(\varepsilon_0 k T_e/q^2 n_e)}$	0.75 mm–4.1 cm	2.2 mm–3.3 cm
r_{ce}	$m_e v_{e,\perp}/q B$	2.15–3.73 cm	25–37 cm
r_{ci}	$m_i v_{i,\perp}/q B$	3.71–6.43 m	Ar:67–100 m

(as low as $\sim 10^{10}$ m^{-3}). If necessary, however, lower densities ($\sim 10^{11}$ m^{-3}) can be obtained in the LVTF farther back from the HCA than this study's measurement space.

One very important aspect of the HCA's plasma environment is that the plasma is uniform over a fairly large region (1–2 m^2). Density and electron temperature vary by only less than a factor of two from side to side and front to back of the measurement space used in this study. In addition, the LVTF's walls are located a large distance from the plasma region of interest, minimizing the confining effects of the walls, often one of the largest problems with simulating an ionospheric plasma. These two aspects allow large and/or distributed systems to be placed in the plasma without requiring compensation for changing conditions across the system. In addition, these aspects allow for the examination of large sheaths, e.g., on high-voltage conductors.[22]

Electron Temperature

The electron temperatures obtained in the study were in the range of $\simeq 0.9$ to 1.8 eV. These values are higher than those found in the ionosphere ($\theta_e \simeq 0.1$ to 0.3 eV), but for many circumstances the difference is not too critical. Electron temperature could possibly be lowered in future experiments by injecting cold gas at the exit of the HCA keeper or by adding polyatomic molecules such as nitrogen to the noble gas HCA propellant. By running a smaller (e.g., 3.2-mm-diam) HCA in spot mode,[15] it may also be possible to achieve lower electron temperatures.

Primary Ion Constituent

The three gases used here—argon, krypton, and xenon—are all heavier than the primary ionospheric constituent: atomic oxygen. In our study we did attempt to use neon, which is close in mass to oxygen, but the cathode ran too hot at the low flow rate required to achieve low densities. For this reason higher flow rates were required, but they produced a much denser plasma than ionospheric levels at 1–2 m from the HCA exit plane. It may be possible to modify the orifice such that the lower flow rates do not overheat the cathode allowing better ion mass matching with neon in future experiments.

Oxygen itself cannot be used as the gas because oxygen "poisons" the porous impregnated tungsten matrix of the HCA, thus preventing or inhibiting electron emission. The presence of oxygen locally oxidizes the matrix material, rendering it sufficiently reactive to creating tungstates with the impregnant compounds.[23] Significant amounts of oxygen hence raise the work function of the matrix to a level where electron emission essentially stops. Thus, gases other than oxygen must be used with the HCA in the chamber.

Magnetic Field

Knowledge of the ambient magnetic field found in the ionosphere and the LVTF is important because it affects several plasma scale lengths and resonance frequencies. The geomagnetic field strength measured in the chamber is about a factor of four smaller than that in the ionosphere. However, this decreased field strength is not necessarily disadvantageous because the addition of Helmholtz coils would allow for varying magnetic field orientations without much interference from the ambient geomagnetic field. For future experiments requiring ambient magnetic fields, we are investigating the possibility of adding Helmholtz coils to the LVTF.

Resonance Frequencies and Scale Lengths

Often what is most important in the experimental simulation of ionospheric plasma is how closely the plasma resonance frequencies and scale lengths are approximated. Resonance frequencies of interest include the electron and ion plasma frequencies ω_{pe} and ω_{pi}; the electron and ion cyclotron frequencies ω_{ce} and ω_{ci}; and the upper and lower hybrid frequencies ω_{uh} and ω_{lh}. Scale lengths of interest include the debye length λ_D and the electron and ion cyclotron radii r_{ce} and r_{ci}. Table 4 summarizes these parameters and gives equations for their derivation along with values for a typical ionosphere and the HCA far field.

By examining the equations for the frequencies and scale lengths given in Table 4, we can determine how closely the values in the HCA plasma environment will approximate those of the ionosphere. In general, the HCA's far-field plasma is good for simulating electron dynamics, but less so for ions. For example, because ω_{pe} depends only on n_e this frequency can be matched closely. Other frequencies that depend on m_i and/or B_0 are not matched as closely but are still reasonably close. With respect to scale length, we see that the electron gyroradius is easily contained within the plasma environment, whereas the ion gyroradius is clearly not contained. In general, the order in which the frequencies occur can be maintained. Finally, because the important λ_D scale length is proportional to $\sqrt{(T_e/n_e)}$, it can be matched very closely.

Nonidealities

Although there are many properties of ionospheric plasma that the far field of the HCA approximates well, it is unable to simulate a plasma flow. Most in situ investigations in the ionosphere are connected to moving spacecraft with orbital velocities high enough that the ion flow is effectively a directed beam. The HCA does not provide such a directed flow, and hence motional effects cannot be readily studied with the HCA in the LVTF.

Uses of the Simulation System

As just demonstrated, the far field of the HCA in a large vacuum chamber approximates an ionospheric plasma in most aspects except plasma flow. One of its most important uses is in facilitating examinations of ionospheric-plasma phenomena in a controlled setting without, in most cases, relying on scaling techniques. This is of obvious importance when testing plasma-diagnostic instruments and the interaction of full-scale spacecraft systems with the plasma environment. The facility has been used, for example, to test the Langmuir probe and spacecraft potential instrument for the ProSEDS mission.[24] Because the electronic control systems of these scientific instruments are developed for certain ranges of densities or frequencies, it is possible to fully test their proper functioning. The facility can also be used to examine nonflow-related sheath structure around full-scale spacecraft systems. Because of the inability to provide a flowing plasma, however, sheath-wake structures cannot be explored.

Another important use of the chamber is in testing scientific instruments that will be used on spacecraft employing electric propulsion (EP) thrusters. The concept here is to verify that the instrument can discern between the ambient (i.e., HCA-generated) plasma and the artificial EP thruster–generated plasma. Future missions will have more and larger ion thrusters firing for long periods of time; improperly designed instruments will not be able to perform their scientific tasks.

Summary

The capability of generating a plasma environment that closely approximates the ionosphere's is useful for examining ionospheric-plasma phenomena in a controlled setting. The data collected and analyzed in this study show that the far-field plasma environment of the HCA approximates ionospheric plasmas. The obtainable density range during this study was between $\sim 10^{12}$ and 10^{13} m^{-3} and higher, but if tests are performed farther back in the LVTF lower densities ($\sim 10^{11}$ m^{-3}) can be obtained. The electron temperatures were in the range of $\simeq$0.9 to 1.8 eV. The plasma parameters varied by only a factor of two from side to side and front to back of the measurement space used in this study.

Acknowledgments

The authors wish to thank Michael Patterson of NASA John H. Glenn Research Center at Lewis Field for the loan of the HCA used in this research. In addition, the authors wish to thank the University of Michigan's Plasmadynamics and Electric Propulsion Laboratory research group and Preston Powell, a 1997 Summer Research Experience for Undergraduates student, for help with the Langmuir-probe analyses.

References

[1]Smith, J., "Low Density Plasma Generation and Measurement" (abstract), *Transactions of the American Geophysical Union*, Vol. 51, No. 11, 1970, p. 785.

[2]Mavrodineanu, R., "Hollow Cathode Discharges," *Journal of Research of the National Bureau of Standards*, Vol. 89, No. 2, 1984, pp. 143–185.

[3]Parks, D. E., Mandell, M. J., and Katz, I., "Fluid Model of Plasma Outside a Hollow Cathode Neutralizer," *Journal of Spacecraft and Rockets*, Vol. 19, No. 4, 1982, pp. 354–357.

[4]Gerver, M. J., Hastings, D. E., and Oberhardt, M. R., "Theory of Plasma Contactors in Ground-Based Experiments and Low Earth Orbit," *Journal of Spacecraft and Rockets*, Vol. 27, No. 4, 1990, pp. 391–402.

[5]Parks, D. E., Katz, I., Buchholtz, B., and Wilbur, P., "Expansion and Electron Emission Characteristics of a Hollow-Cathode Plasma Contactor," *Journal of Applied Physics*, Vol. 74, No. 12, 1993, pp. 7094–7100.

[6]Conde, L., León, L., and Ibáñez, L. F., "Electron Transport Properties of Stationary Plasma Clouds Generated with Hollow Cathode Discharges," *IEEE Transactions on Plasma Science*, Vol. PS-25, No. 4, 1997, pp. 548–552.

[7]Williams, J. D., and Wilbur, P. J., "Experimental Study of Plasma Contactor Phenomena," *Journal of Spacecraft and Rockets*, Vol. 27, No. 6, 1990, pp. 634–641.

[8]Hastings, D. E., "Theory of Plasma Contactors Used in the Ionosphere," *Journal of Spacecraft and Rockets*, Vol. 24, No. 3, 1987, pp. 250–256.

[9]Parks, D. E., and Katz, I., "Theory of Plasma Contactors for Electrodynamic Tethered Satellite Systems," *Journal of Spacecraft and Rockets*, Vol. 24, No. 3, 1987, pp. 245–249.

[10]Iess, L., and Dobrowolny, M., "The Interaction of a Hollow Cathode with the Ionosphere," *Physics of Fluids B*, Vol. 1, No. 9, 1989, pp. 1880–1889.

[11]Vannaroni, G., Dobrowolny, M., Melchioni, E., Venuto, F. D., and Giovi, R., "Characterization of the Interaction Between a Hollow Cathode Source and an Ambient Plasma," *Journal of Applied Physics*, Vol. 71, No. 10, 1992, pp. 4709–4717.

[12]Gallimore, A. D., Kim, S.-W., Foster, J. E., King, L. B., and Gulczinski, F. S., III, "Near and Far Field Plume Studies of a One-Kilowatt Arcjet," *Journal of Propulsion and Power*, Vol. 12, No. 1, 1996, pp. 105–111.

[13]Sarver-Verhey, T. R., "Continuing Life Test of a Xenon Hollow Cathode for a Space Plasma Contactor," NASA CR-195401, Nov. 1994.

[14]Rawlin, V. K., and Pawlik, E. V., "Mercury Plasma-Bridge Neutralizer," *Journal of Spacecraft and Rockets*, Vol. 5, No. 7, 1968, pp. 814–820.

[15]Domonkos, M. T., Gallimore, A. D., and Patterson, M. J., "Low-Current Hollow Cathode Evaluation," AIAA Paper 99-2575, June 1999.

[16]Rawlin, V. K., "A 13,000 Hour Test of a Mercury Hollow Cathode," NASA TM X-2785, June 1973.

[17]Bilén, S. G., Domonkos, M. T., and Gallimore, A. D., "The Far-Field Plasma Environment of a Hollow Cathode Assembly," AIAA Paper 99-2861, June 1999.

[18]Krehbiel, J. P., Brace, L. H., Theis, R. F., Pinkus, W. H., and Kaplan, R. B., "The Dynamics Explorer Langmuir Probe Instrument," *Space Science Instrumentation*, Vol. 5, No. 4, 1981, pp. 493–502.

[19]Agüero, V., Banks, P. M., Gilchrist, B., Linscott, I., Raitt, W. J., Thompson, D., Tolat, V., White, A. B., Williams, S., and Williamson, P. R., "The Shuttle Electrodynamic Tether System (SETS) on TSS-1," *Il Nuovo Cimento*, Vol. 17C, No. 1, 1994, pp. 49–65.

[20]Barton, C. E., "International Geomagnetic Reference Field: The Seventh Generation," *Journal of Geomagnetism and Geoelectricity*, Vol. 49, No. 2–3, 1997, pp. 123–148.

[21]Bozorth, R. M., *Ferromagnetism*, Van Nostrand, New York, 1951, pp. 147–149.

[22]Bilén, S. G., "Pulse Propagation Along Conductors in Low-Density, Cold Plasmas as Applied to Electrodynamic Tethers in the Ionosphere," Ph.D. Dissertation, Electrical Engineering, Univ. of Michigan, Ann Arbor, MI, Sept. 1998.

[23]Ohlinger, W. L., and Rebstock, K. M., "Barium Calcium Almuminate Impregnant Materials: Interaction with Sea-Level Ambient Atmospheres and Decomposition Behaviors of Reaction Products," AIAA Paper 94-3135, June 1994.

[24]Johnson, L., Gilchrist, B. E., Estes, R. D., Lorenzini, E., and Ballance, J., "Propulsive Small Expendable Deployer System (ProSEDS) Space Experiment," AIAA Paper 98-4035, June 1998.

A. C. Tribble
Associate Editor